ISSN: 2664-9640

Boron-doped MXene cathode materials for Lithium-Sulfur batteries

Haodong Yin [a], YeLi Yan [b], Zhibin Wang [c], Peibo Shi [d], and Fanghao Li [e]

School of Shangdong, Jiaotong University, Weihai 264210, China;

[a]1290450002@qq.com, [b]Lyer1210@126.com, [c]wzb1786297922@163.com, [d]1014418900@qq.com, [e]772749373@qq.com

Abstract

Lithium-sulfur(L-S) batteries have extremely high theoretical capacity and energy density, making them one of the most promising energy storage systems. However, the severe shuttle effect and the rapid capacity fading and low practical energy density caused by the poor conductivity of the sulfur cathode have hindered its development. Rational cathode material design is one of the effective strategies to solve the above problems. Herein, by using boric acid (H_3BO_3) as the boron source, boron-doped MXene composite cathode material B-$Ti_3C_2T_x$ was prepared by a hydrothermal method for application in lithium-sulfur batteries. The prepared cathode material was characterized and its electrochemical properties were tested, The experimental results show that B-$Ti_3C_2T_x$ retains the advantages of high specific surface area and pore volume of $Ti_3C_2T_x$ 2D material, and the doping of boron further improves the conductivity of the cathode material and the adsorption performance of polysulfide. The sulfur content in the B-$Ti_3C_2T_x$/S is as high as 70.2%, and the initial discharge specific capacity of 1055.5 mAh·g^{-1} obtained at 0.2 C rate current and remained at 755.3 mAh·g^{-1} after 100 cycles, which was 71.6% of the intital discharge capacity. The B-$Ti_3C_2T_x$ electrode idea proposed in this paper provides a reference for realizing low-cost and high-energy-density Li-S batteries.

Keywords

Lithium-sulfur batteries , shuttle effect, Ti3C2Tx-MXene, element doping.

1. Introduction

With the increasingly serious problems of environmental degradation and increasing energy demand, renewable energy and devices have been rapidly developed. In order to reduce the use of fossil fuels, people have begun to pay extensive attention to the development of clean and renewable energy such as solar energy and wind energy. However, such renewable energy has inherent characteristics such as variability and intermittency, and requires the cooperation of energy storage systems [1]. Therefore, it is particularly important to develop new and efficient energy storage systems. Among them, lithium- ion batteries are widely used in various related fields because of their high energy density, long cycle life, and no memory effect . However, with the increase in energy demand, lithium-ion batteries have been unable to meet the current demand for high energy density systems. Therefore, the development of energy storage systems with higher specific capacity and lower cost is of great significance to sustainable development [2].

Lithium-sulfur (Li-S) batteries has extremely high theoretical specific capacity (1675 mAh·g^{-1}) and energy density (2500 Wh·kg^{-1}), and has the advantages of abundant resources, low cost and environmental friendliness. It is considered to be one of the most promising electrochemical energy storage devices [3]. Nevertheless, despite the significant advantages of

ISSN: 2664-9640

Li-S batteries, the realization of their commercial applications is still hindered by problems such as rapid capacity fading, low actual energy density, and poor cycle life. The main reasons for these problems are the shuttle effect of polysulfides and the poor conductivity of sulfur. Therefore, designing a solution to effectively inhibiting the shuttle effect and improves the conductivity is the key to promote the rapid development of lithium-sulfur batteries.

Extensive research have shown that developing suitable cathode composites is one of the effective solutions [4]. For example, carbon materials doped with heteroatoms such as N, B, Co, etc, can enhance the conductivity of carbon materials and the adsorption performance of polysulfides, thereby improving the cycle performance of batteries [5]. Sun et al [6] prepared a gelatin nitrogen doped porous carbon cathode with large pore volume, andits initial discharge capacity as high as 1384 $mAh \cdot g^{-1}$ at 1 C and remains at 700 $mAh \cdot g^{-1}$ after 100 cycles, which is higher than that of the comparison material undoped nitrogen -element. Xu et al [7] obtained a boron doped carbon nanotube and sulfur composite cathode material (BUCNTs/S) by a hydrothermal one-pot method. The experimental liquid phase in-situ synthesis made the sulfur distribution in the composite more uniform, While boron doping endows carbon-based host materials with higher electrical conductivity and stronger sulfur fixation ability. Compared with nitrogen doping, which is more electronegative than carbon, the electronegativity of boron is weaker than that of carbon, and as an electron deficient element, boron doping is considered to have natural advantages in improving the conductivity and sulfur fixation of carbon materials. The solution of heteroatom doping provides beneficial inspiration for improving the performance of Li-S batteries. In recent years, Gogotsi's group has discovered a new 2D transition metal carbon/nitride—$Ti_3C_2T_x$ MXene materials [8], which shows great potential in the field of Li-S batteries because of its abundant surface functional groups, unique 2D structure, and higher electrical conductivity [9]. Wang et al. [10] used MXene powders as sulfur carrier materials and proved that MXenes could utilize the Lewis acid-base mechanism to form strong Ti–S bonds to capture polysulfides. These studies proved that Mxene has excellent effect as a cathode sulfur-carrying material.

Different from the above related studies. Herein, by using boric acid (H_3BO_3) as the boron source, boron-doped MXene composite cathode material B-$Ti_3C_2T_x$ was prepared by a hydrothermal method, The electronegativity of B element is smaller than that of C element, so it is positive after doping into the MXene group, which is conducive to the strong charge adsorption with polysulfide anions, thereby effectively inhibiting the shuttle effect, and the doping of B element can effectively increase the MXene nanosheets pore volume and specific surface area, while enhancing the conductivity of the cathode material and promoting the reaction kinetics.

2. Experimental section

2.1. Reagents and instruments

Sublimation sulfur (analytical reagen, Chengdu Kelong Chemical Co., Ltd.), Lithium fluoride (analytical reagen, Tianjin Jinhui Taiya Chemical Reagent Co., Ltd.), Titanium aluminum carbide (99.5%, Foshan Xinene Technology Co., Ltd.), Concentrated hydrochloric acid (analytical reagen, Yantai Shuangshuang Chemical Co., Ltd.), Boric acid (analytical reagen, Yantai Shuangshuang Chemical Co., Ltd.), Polypropylene film (battery grade, Shenzhen Tianchenghe Technology Co., Ltd.), Polyvinylidene fluoride (battery grade, Dongguan Zhanyang Polymer Materials Co., Ltd.), N - methylpyrrolidone (analytical reagen, Tianjin Beilian Fine Chemicals Development Co., Ltd.)

The microstructure of the material was observed by scanning electron microscope (SEM), the crystal structure of the material was detected by X-ray diffractometer (XRD), the sulfur content was determined by thermogravimetric analysis (TGA), and the wettability of electrode and electrolyte was determined by the contact angle of water droplet. The specific capacity, rate

ISSN: 2664-9640

performance and impedance of the battery are tested by constant current charge and discharge test, cyclic voltammetry (CV), and alternating current impedance test (EIS).

2.2. $Ti_3C_2T_x$ Preparation

First, add 1 g LiF to 20 mL HCl (9 mol·L^{-1}) and stir until completely dissolved. Then, 1 g Ti_3AlC_2 powder was slowly added to the mixed solution, placed at 35°C for continuous stirring for 24 h, and the obtained suspension was washed with deionized water for several times by centrifugation(3500 r·min^{-1} , 5 min each time) until the pH of the supernatant is close to neutral. Then, the precipitate was dispersed in deionized water by ultrasonic dispersion for 1.5 h, and then centrifuged at 3500 r·min-1 for 1 h to collect the dark green upper layer solution, which was the $Ti_3C_2T_x$ dispersion. Freeze-dry the upper layer solution to obtain $Ti_3C_2T_x$ powder.

2.3. B-$Ti_3C_2T_x$/S Preparation

Add 1.5 g of H_3BO_3 to 80 mL $Ti_3C_2T_x$ dispersion and sonicate for 30 min. The mixed solution was transferred to a 100 mL Teflon-lined autoclave, and the hydrothermal reaction was carried out at 180°C for 12 h. After the reaction, the obtained product was repeatedly washed with deionized water, and then dried in vacuum at 60℃ for 12 h. Finally, a B-$Ti_3C_2T_x$ complex was obtained.

The B-$Ti_3C_2T_x$/S composite material adopts the melt diffusion method, and the B-$Ti_3C_2T_x$ composite and sulfur are mixed in a mass ratio of 1:2. The mixture was then added to a drying oven at 155°C and held for 12 h, then raised to 300℃ and kept for 2 h. After cooling to room temperature, a B-$Ti_3C_2T_x$/S composite material was obtained. In order to compare with $Ti_3C_2T_x$ powder only, $Ti_3C_2T_x$/S composites were prepared by the same method.

2.4. Assemble the battery

B-$Ti_3C_2T_x$/S, acetylene black and PVDF were uniformly mixed in NMP at a mass ratio of 8:1:1 to make a cathode paste, evenly coat the obtained paste on the aluminum foil, dry it in a vacuum oven at 60℃ for 12 h, then cut into a round piece(diameter=12 mm), weigh the mass of the cathode pieces, and put it in a glove box for standby.

The battery is assembled in an argon atmosphere glove box with both water and oxygen content less than 1 ppm. Use CR2025 model shell, use 16×0.4 mm metal lithium sheet is used as the anode, the Celgard 2400 PP diaphragm is used as the diaphragm, the mixed solution of DME and DOL is prepared according to the volume ration of 1:1, use 1 M LiTFSI as the lithium salt, and adds 0.1 M $LiNO_3$. Place the cathode sheet in the middle of the cathode shell and add the electrolyte. After the cathode sheet is completely wet, put it into the separator and add the electrolyte solution again. Place the metal lithium sheet, gasket, shrapnel, and battery case on the separator in turn, and then use a sealing machine. Seal the battery and let the assembled battery stand for 12 h.

2.5. Li_2S_6 adsorption experiment

Li_2S and sublimation sulfur were dissolved in a DOL/DEM (volume ratio 1:1) mixed solution at a molar ratio of 1:5, and then stirred at 60°C for 12 h to obtain a Li_2S_6 solution. Add $Ti_3C_2T_x$ and B-$Ti_3C_2T_x$ to a small glass bottle containing 3 mL of Li_2S_6 solution and let it stand for 12 h. Observe the color change of the solution to determine the adsorption of polysulfides.

3. Results and discussion

3.1. Morphology and phase analysis of materials

Using Ti_3AlC_2 as a precursor, it is processed in a LiF/HCI mixed solution to etch the Al atomic layer. The multi-layer $Ti_3C_2T_x$ obtained by etching is then ultrasonically peeled off, and then freeze-dried to obtain a few-layer flaky $Ti_3C_2T_x$ powder. As can be seen in Fig. 1a, the initial

ISSN: 2664-9640

Ti_3AlC_2 morphology is a layered structure of bulk particles, and the $Ti_3C_2T_x$ obtained after etching treatment is shown in Fig. 1b, showing a wrinkled flakes, the interlayer spacing increases significantly. The topography of B-$Ti_3C_2T_x$ is shown in Fig. 1c. It can be clearly seen from the image that the layered stack structure of $Ti_3C_2T_x$ is not damaged by the doping of boron element, and it perfectly inherits the 2D shape structure of $Ti_3C_2T_x$ sheet. At the same time, its active sites are not blocked by boron doping. The tiny 2D structure can enable the rapid diffusion of lithium ions and shorten the distance of the electron transfer channel in the cathode, realizing the rapid transfer of cathode electrons.

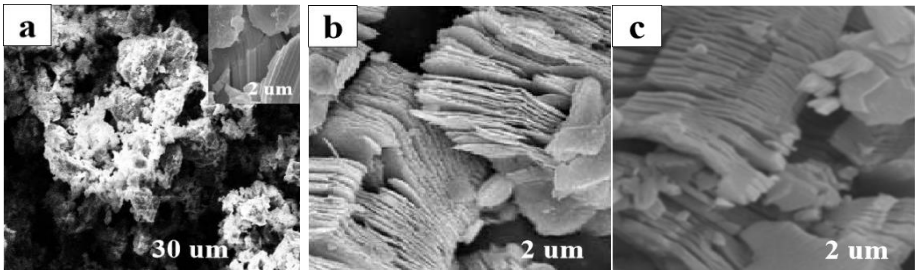

Fig. 1 SEM of (a) Ti_3AlC_2, (b) $Ti_3C_2T_x$ and (c) B-$Ti_3C_2T_x$

In order to further analyze the structural gap between $Ti_3C_2T_x$ and B-$Ti_3C_2T_x$, we obtained XRD patterns of $Ti_3C_2T_x$ and B-$Ti_3C_2T_x$ by means of X- ray diffractometer, as shown in Fig. 2. The main crystal phase peak (002) of MXene is evident in both XRD patterns, which indicates that the structure of $Ti_3C_2T_x$ is not damaged, which is consistent with the SEM observation. Compared with the (002) characteristic diffraction peak of $Ti_3C_2T_x$ located at 6.8°, the (002) characteristic diffraction peak of B-$Ti_3C_2T_x$ is shifted, and it is displayed at about 6.3° of the (002) diffraction surface of MXene, which means that $Ti_3C_2T_x$ enlarges the interlayer spacing of the nanosheets after boron element doping treatment , and the structure is well preserved.

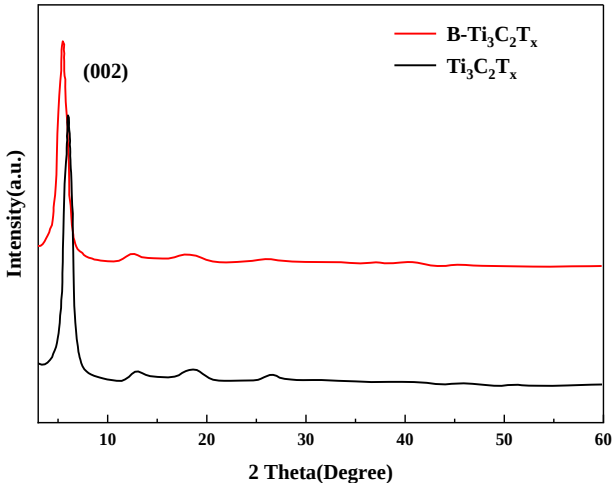

Fig. 2 XRD patterns of $Ti_3C_2T_x$ and B-$Ti_3C_2T_x$

3.2. Structural performance analysis of materials

In order to study the contact performance between material and electrolyte, the contact angles of $Ti_3C_2T_x$ and B-$Ti_3C_2T_x$ to the electrolyte were tested. According to the test results in Fig. 3, it was found that the angles angles obtained by $Ti_3C_2T_x$ are 29° (Fig. 3a) and 12.6° (Fig. 3b). The above data show that the affinity between B-$Ti_3C_2T_x$ and the electrolyte is the best . Therefore, when B-$Ti_3C_2T_x$ is used as the cathode material, the electrolyte in the battery can be greatly retained and the internal resistance of the battery can be reduced , which is beneficial to reduce the internal resistance of the electrode and improve the electrochemical performance.

ISSN: 2664-9640

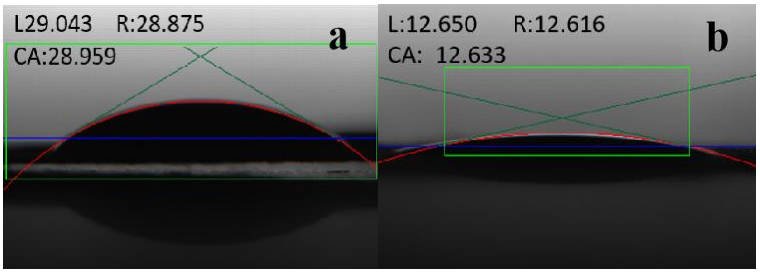

Fig. 3 Contact angle of (a) $Ti_3C_2T_x$ and (b) B-$Ti_3C_2T_x$

The doping of B element increases the specific surface area of $Ti_3C_2T_x$ and forms a unique structural advantage, which indicates that it can effectively improve the adsorption capacity of polysulfides. To visually verify this result, we studied the adsorption effects of $Ti_3C_2T_x$ and B-$Ti_3C_2T_x$ on polysulfides (Li_2S_6). As shown in Fig. 4, it can be clearly observed that after standing for 12 h, the colors of both $Ti_3C_2T_x$ (B) and B-$Ti_3C_2T_x$ (C) solutions has becom shallow, but in contrast, the solution of B-$Ti_3C_2T_x$ is nearly colorless , which proves that B doping further enhances the ability of $Ti_3C_2T_x$ to adsorb polysulfides.

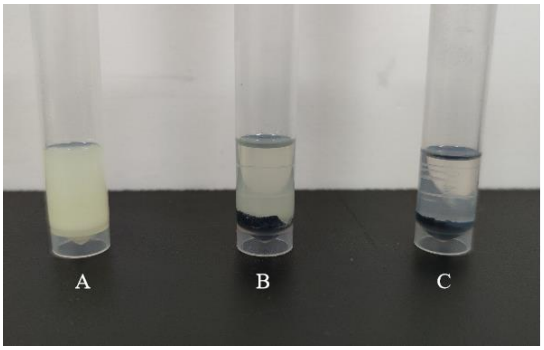

Fig. 4 Li_2S_6 solution adsorption of $Ti_3C_2T_x$ and B-$Ti_3C_2T_x$

Through the thermogravimetric analysis (TGA) test, the sulfur content in the two composites , $Ti_3C_2T_x$/S and B-$Ti_3C_2T_x$/S , was 64.3 wt % and 70.2 wt % , respectively, as shown in Fig. 5. It is also demonstrated that B doping has a larger specific surface area and pore volume, and it is proved that the existence of B element enhances the adsorption of sulfur to a certain extent.

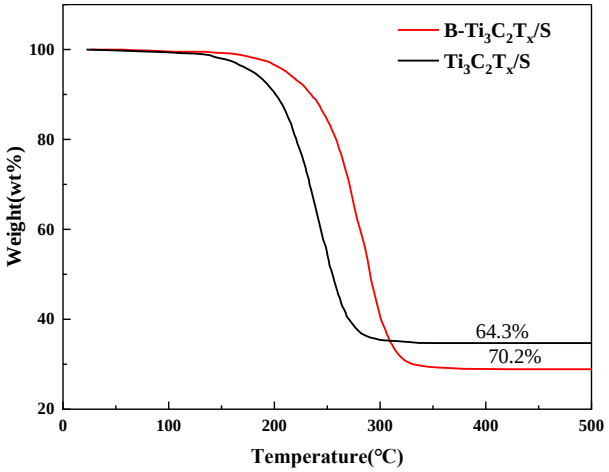

Fig.5 TGA curves of $Ti_3C_2T_x$/S and B-$Ti_3C_2T_x$/S

3.3. Electrochemical and test analysis

To evaluate the electrochemical performance of the composites, the prepared different electrodes were assembled into coin cells for electrochemical tests. Fig. 6a shows the Cyclic voltammetry (CV) curves of $Ti_3C_2T_x$/S and B-$Ti_3C_2T_x$/S electrodes at a scanning rate of 0.1 $mV \cdot S^{-1}$ in the voltage window of 1.7-2.8 V. Two reduction peaks and one oxidation peak can be clearly observed in the figure, the two reduction peaks are related to the typical multi-stage reduction

ISSN: 2664-9640

process of sulfur, that is, the transformation of solid sulfur to liquid long-chain polysulfides and further reduction of liquid long-chain polysulfides to solid Li_2S_2/Li_2S. The oxidation peaks correspond to the transformation of Li_2S/Li_2S_2 into polysulfides and finally into sulfur [11]. Comparing the two electrodes, it can be seen that the redox peak spacing of the B-$Ti_3C_2T_x$/S electrode becomes smaller and has a higher peak intensity, which indicates that the doping of B reduces the electrode polarization and reduces the electrode polarization and inproves the reaction kinetics of the electrode.

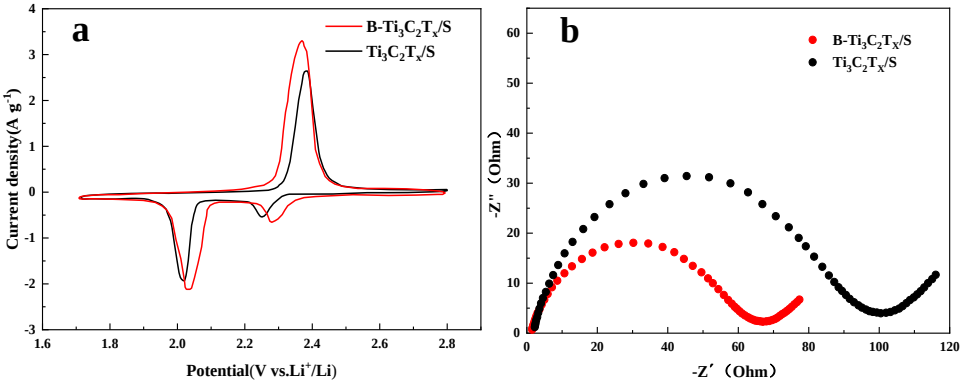

Fig.6 (a) CV curves and (b) Nyquist plots of $Ti_3C_2T_x$/S and B-$Ti_3C_2T_x$/S electrodes

In order to compare the charge-discharge performance and cycle performance of $Ti_3C_2T_x$/S and B- $Ti_3C_2T_x$/S electrodes, we first tested the constant current charge-discharge at 0.2 C rate current. The results are shown in Fig. 7a-b , from which it can be seen that the curves have two discharge plateaus at approximately 2.3 and 2.1 V, which are related to the reduction of sulfur to long-chain polysulfides and the further transformation to solid-state Li_2S_2/Li_2S, which is consistent with the above CV curve results. Lithium polysulfide is in turn converted to sulfur at the charging platform of 2.3-2.4 V [12]. In addition, it can also be seen from the figure that the discharge specific capacity of the B-$Ti_3C_2T_x$/S electrode is higher than that of the $Ti_3C_2T_x$/S electrode (1055.5 mAh·g^{-1} and 898.4 mAh·g^{-1} respectively), and the polarization of the B-$Ti_3C_2T_x$/S electrode is smaller than that of the $Ti_3C_2T_x$/S electrode. The higher specific capacity and lower polarization of the B-$Ti_3C_2T_x$/S electrode is due to the doping of born element that effective anchors and reuse polysulfides to improve the utilization rate of sulfur, as well as the higher battery reaction kinetics, which is consistent with the result of higher redox peaks appearing in the CV curves. In addition, as shown in Fig. 8, the B-$Ti_3C_2T_x$/S electrode exhibited more excellent cycling stability in the cyclic charge-discharge test, After 100 cycles, the discharge specific capacity of the B-$Ti_3C_2T_x$/S electrode is 755 mAh·g^{-1}, which is 71.6% of the initial specific capacity, which is better than the discharge specific capacity of 592 mAh·g^{-1} and the retention rate of 65.9 % of the $Ti_3C_2T_x$ /S electrode.

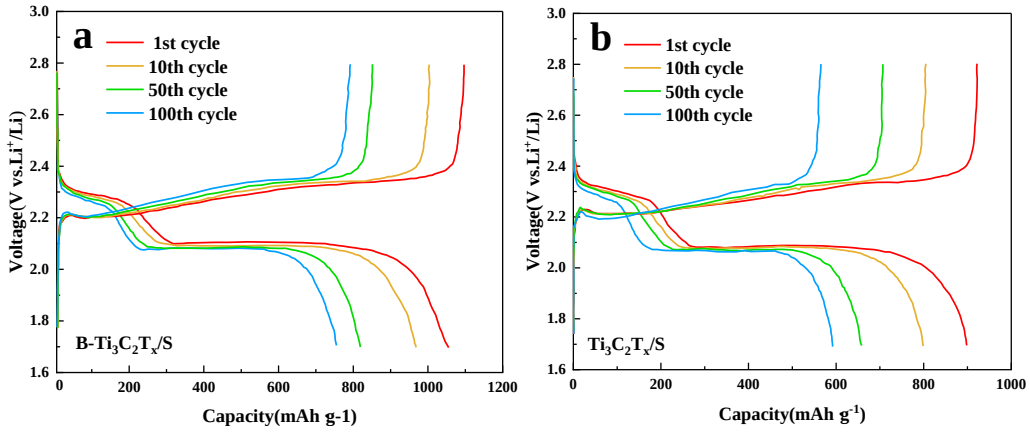

Fig. 7 Charge/discharge curves of(a) $Ti_3C_2T_x$/S and (b) B-$Ti_3C_2T_x$/S electrodes at 0.2 C

ISSN: 2664-9640

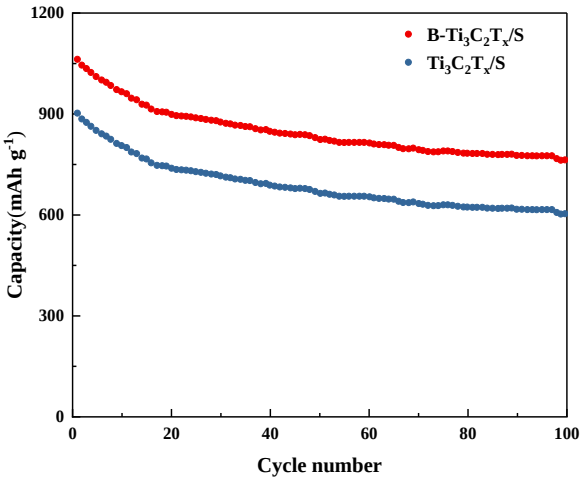

Fig. 8 cycling performance of $Ti_3C_2T_x$/S and B-$Ti_3C_2T_x$/S electrodes at 0.2 C

We tested the discharge specific capacity of $Ti_3C_2T_x$/S and B-$Ti_3C_2T_x$/S electrodes at different current densities of 0.2, 0.5, 1, 2, and 5 C continuously varying, as shown in Fig. 9. The discharge specific capacities of the B-$Ti_3C_2T_x$/S electrode at different rates are 1053.5, 924.9, 806.5, 714.6, 482.3 mAh g^{-1}, and after the current density is suddenly changed to 0.2 C, the B-$Ti_3C_2T_x$/S electrode can still reaches 879.4 mAh·g^{-1}. However, at the same test rate, the discharge specific capacities of $Ti_3C_2T_x$/S electrodes were 897.3, 769.8, 671.5, 528.9, 325.3 and 705.1 mAh·g^{-1}, respectively. In contrast, the B- $Ti_3C_2T_x$/S electrode has higher specific discharge capacity at different rates, which proving that the boron-doped B-$Ti_3C_2T_x$/S electrode has better rate performance and cycle stability.

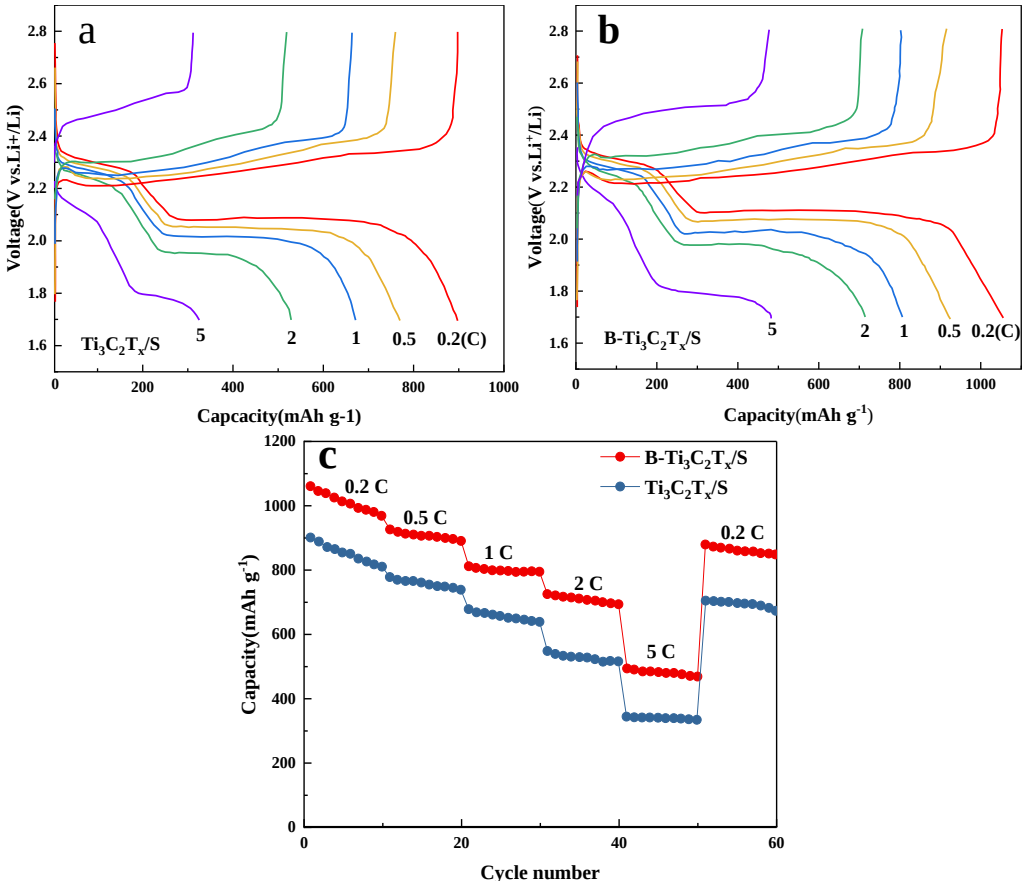

Fig. 9 (a) Charge-discharge curves of $Ti_3C_2T_x$/S, (b) B-$Ti_3C_2T_x$/S electrodes at various rates, and (c) Rate capability

ISSN: 2664-9640

4. Conclusion

We report that the successful preparation of boron-doped MXene B-$Ti_3C_2T_x$ as a cathode composite by a hydrothermal method using H_3BO_3 as the boron source. B-$Ti_3C_2T_x$ material retains the advantages of large specific surface area and pore volume of $Ti_3C_2T_x$ material itself, and does not block active sites, which not only effectively improves the diffusion of lithium ions, but also shortens the electron transfer distance and promotes the reaction kinetics.

The structural property analysis of the material shows that the doping of B element enhances the inhibition of polysulfide adsorption, and the sulfur content in the composite material is as high as 70.2%. The B-$Ti_3C_2T_x$/S electrode achieved excellent electrochemical performance: an initial discharge specific capacity of 1055.5 mAh·g^{-1} was obtained at 0.2 C, which remained at 755.3 mAh·g^{-1} after 100 cycles, which is 71.6% of the initial discharge capacity, the discharge specific capacity of the $Ti_3C_2T_x$/S electrode, with excellent rate performance and cycle stability. The strategies and experimental results presented in this paper provide a reference scheme for improving the energy density of Li-S batteries.

Acknowledgements

This work was funded by National Natural Science Foundation of China (51609131); Introduction and Education Plan of Young Creative Talents in Universities of Shandong Province(500076); Demonstration Base of Joint Cultivation of Graduate Students in Shandong Province. Shandong Jiaotong University “Climbing” Research Innovation Team Program (SDJTUC1802); Key research and development plan in Shandong Province(2019GHY112018); Shandong Provincial Higher Educational Science and Technology Foundation, China (KJ2018BBA015).

References

[1] Y. Li, S. Guo: Material design and structure optimization for rechargeable lithium-sulfur batteries, Matter, Vol. 4 (2021) No.4, P.1142-1188.

[2] M. Zhao, B.Q. Li, X.Q. Zhang, et al: A perspective toward practical lithium–sulfur batteries, ACS Central Science, Vol. 6 (2020) No.7, P.1095-1104.

[3] J. Wang, S. Yi, J. Liu, et al: Suppressing the shuttle effect and dendrite growth in lithium–sulfur batteries, ACS nano, Vol. 14 (2020) No.8, P. 9819-9831.

[4] J.H. Zuo, Y.J. Gong: Applications of transition-metal sulfides in the cathodes of lithium–sulfur batteries, Tungsten, Vol. 2 (2020) No. 2, P.134-146.

[5] Y. Lu, H.J. Shi, Y.F. Su, et al: Application of Element-Doped Carbonaceous Materials in Lithium-Sulfur Batteries, Progress in Chemistry, Vol. 33, (2021) No.9, P.1598-1613.

[6] C. Sun, D. Guo, Q. Shao, et al: Preparation of gelatin-derived nitrogen-doped large pore volume porous carbons as sulfur hosts for lithium-sulfur batteries, New carbon materials, Vol. 36, (2021) No.1, P.198-208.

[7] C. Xu, H. Zhou, C. Fu, et al: Hydrothermal synthesis of boron-doped unzipped carbon nanotubes/sulfur composite for high-performance lithium-sulfur batteries, Electrochimica Acta, Vol. 232, (2017) No.4, P.156-163.

[8] M. Naguib, M. Kurtoglu, V. Presser, et al: Two-dimensional nanocrystals produced byexfoliat ion of Ti3AlC2, Advanced Materials, Vol. 23, (2011) No.37,P.4248-4253.

[9] Q. Zhao, Q. Zhu, Y. Liu, et al: Status and Prospects of MXene-Based Lithium-Sulfur Batteries, Advanced Functional Materials, Vol.31, (2021) No.21,P.1-28.

[10] X. Wang, C. Yang, X. Xiong, et al: A robust sulfur host with dual lithium polysulfide immobilization mechanism for long cycle life and high capacity Li-S batteries,Energy Storage Materials, Vol. 16, (2019) No.1, P.344-353.

ISSN: 2664-9640

[11] K. Wu, Y. Hu, Z. Shen, et al: Highly efficient and green fabrication of a modified C nanofiber interlayer for high-performance Li–S batteries, Journal of Materials Chemistry A, Vol. 6, (2018) No.6, P.2693-2699.

[12] X Zhang, K Chen, Z Sun, et al: Structure-related electrochemical performance of organosulfur compounds for lithium–sulfur batteries, Energy & Environmental Science, Vol. 16, (2020) No.4, P.1076-1095.